Available online at www.sciencedirect.com
ScienceDirect
Bioelectrochemistry 72 (2008) 41–46
Bioelectrochemistry
www.elsevier.com/locate/bioelechem

Magnetic fields of 10mT and 120mT change cell shape and structure of F-actins of periodontal ligament cells

Chun Xu [a], Zhen Fan [b], Yong-Lie Chao [c,*], Li Du [c], Fu-Qiang Zhang [a]

[a] *Department of Prosthodontics, Affiliated Ninth People's Hospital, Medical School, Shanghai Jiao Tong University, Shanghai 200011, China*
[b] *Department of Prosthodontics, Affiliated Stomatological Hospital, Tongji University, Shanghai 200072, China*
[c] *Department of Prosthodontics, West China Stomatological Hospital, Sichuan University, Chengdu 610041, China*

Received 7 July 2007; received in revised form 28 October 2007; accepted 16 November 2007
Available online 24 November 2007

Abstract

Dental magnetic attachments, usually applied locally to oral cavities, produce stray fields (flux leakage) spreading in adjacent tissues. It has been found that human periodontal ligament (PDL) cells change their geometry and the structure of their cytoskeleton F-actins when the cell cultures are exposed to *B*-field strengths of B = 10mT and 120mT, respectively, which are similar to those generated by dental magnetic attachments. Analytically, after long-time exposures to *B*-fields for 12h, 36h and 60h, respectively, cytoskeleton F-actins are labeled with a fluorescent dye and observed under a laser scanning confocal microscope. The geometrical cell parameters of cell length and cell width and the fluorescence emission of labeled F-actins, respectively, were determined and subjected to an automatic image analysis using a special software. The results on cell shrinkage and filament reorganizations were statistically analyzed by the program ANOVA ($P < 0.05$). It was found that only long-time (hours) exposure to high fields in the order of 0.1T may produce tissue irritations during long-time medical treatments using open- and closed-field dental magnetic attachments.

Keywords: Magnetic dental attachment; Static magnetic *B*-fields; Periodontal ligament cell; Cytoskeleton; Confocal fluorescence microscopy

1. Introduction

There is appreciable continuous public concern on potential health hazards from technical electromagnetic field (EMF) radiations experienced in daily life of our civilization. The targets of concern are the high voltage power transmission lines, industrial machines, household appliances, communication equipments and medical electromagnetic instruments, including NMR devices, in the diagnosis and during treatment of diseases [1–4].

Specifically, magnetic fields are also used in clinical prosthodontics. Several types of dental magnetic attachments have been applied to aid the retention of prosthesis with claimed "favorable effects" [5]. Dental magnetic attachments utilize the static magnetic field generated by strong permanent magnets to aid the retention and stability of dentures. Early magnetic attachments are of the open-field type and have relatively small retentive forces. The most frequently used magnetic attachments are of the closed-field type, which are composed of Nd2Fe14B magnets with "yokes and keepers" of soft magnetic alloy.

In 1979, Wertheimer and Leeper reported that children resided near transmission lines had 2 to 3 times higher risk of cancer occurrences [6]. Their report revived appreciable attentions on potential biological effects of even small magnetic fields and small exposure time. There are many reports and claims on beneficial effects as well as negative EMF effects on all kinds of biological materials [7–10]. Many of the claims of biological effects of magnetic *B*-fields are hardly biophysically rationalizable and are thus controversially discussed [11–25].

In the context of medical *B*-field treatments, both the open-field and the closed-field dental magnetic attachments produce stray fields, called flux leakages, spreading to the adjacent tissues, for instance, when locally used in the oral cavity [5,26].

Presently there are few reports about the biological effects of *B*-fields generated by magnetic attachments on human tissues

* Corresponding author. Fax: +86 21 63135412.
E-mail address: imxuchun@163.com (Y.-L. Chao).

1567-5394/$ - see front matter © 2007 Elsevier B.V. All rights reserved.
doi:10.1016/j.bioelechem.2007.11.009

and, in vitro, on cell cultures. We previously reported that *B*-fields, similar in intensity to those generated by dental magnetic attachments, lead to changes in the cell morphology and proliferation of human periodontal ligament (PDL) cells [27]. These *B*-fields obviously affect the cytoskeleton filaments, which are known as key components in maintaining the overall shape of cells [11,28,29].

The present study reports that *B*-fields and long exposure time cause cell shrinkage and structural reorganizations of the cytoskeleton F-actins in human PDL cells. The applied fields are comparable to those generated by dental magnetic attachments.

2. Materials and methods

2.1. Cell culture

Human PDL cells were isolated from the ligament tissues of a periodontally healthy, non-carious human tooth extracted for orthodontic reason from one donor (14-year-old male) with informed consent. The cells were maintained and expanded in Dulbecco's Modified Eagle's Medium (DMEM, Gibco, Grand Island, NY, USA) supplemented with 10% fetal bovine serum (FBS, Hyclone Laboratories, Logan, UT, USA) and antibiotics (100U ml^{-1} penicillin, 100μg ml^{-1} streptomycin). PDL cells were used in these experiments at passage 5 to 6.

2.2. Magnetic exposure

A cellular *B*-field exposure system utilizing arrays of Nd2Fe14B permanent magnets has been developed by the authors. It consists of 5 components: array of permanent magnets, pedestal, loading platform, vernier scale and magnetic shield (Fig. 1).

Cell culture dishes were placed on the loading platform above the magnetic array and cells cultured on the dishes were exposed the *B*-fields. The distance between the loading platform and the array was adjustable. Because the *B*-fields around magnets decrease with distance from the surfaces of the magnets [30], the *B*-field strength is adjusted via altering the height of the loading platform. Based on previous results, obtained with two commonly used commercial magnetic attachments (Magfit EX600W and Magnedisc 800, Aichi steel Co. Ltd, Japan) [26], the specifications of B = 10mT and B = 120mT were selected, to simulate the conditions of the closed-field and the open-field magnetic attachments, respectively.

Human PDL cells were plated on 60mm culture dishes at a concentration of 2×10^5 cells/dish and cultured in a CO_2 incubator (Model MCO-15AC, Sanyo electric Co. Ltd, Japan) at 37°C in a humidified 5% CO_2 atmosphere. After 3days of cultivation, PDL cells were exposed to B = 10mT and to B = 120mT, respectively, each for 12h, 36h and 60h, respectively, 12h per day; the exposure system is located in the CO_2 incubator. The mode of 12h exposure per day is to simulate the clinical situation of magnetic attachment denture, which is worn by patients only during day time. Control cells were cultured outside of the exposure system in the CO_2 incubator at 37°C in a humidified 5% CO_2 atmosphere and were exposed to geomagnetic fields in the range of $0.03 \leq B/\mathrm{mT} \leq 0.07$, as measured with a digital Teslameter (Model 7010, F.W.Bell, USA).

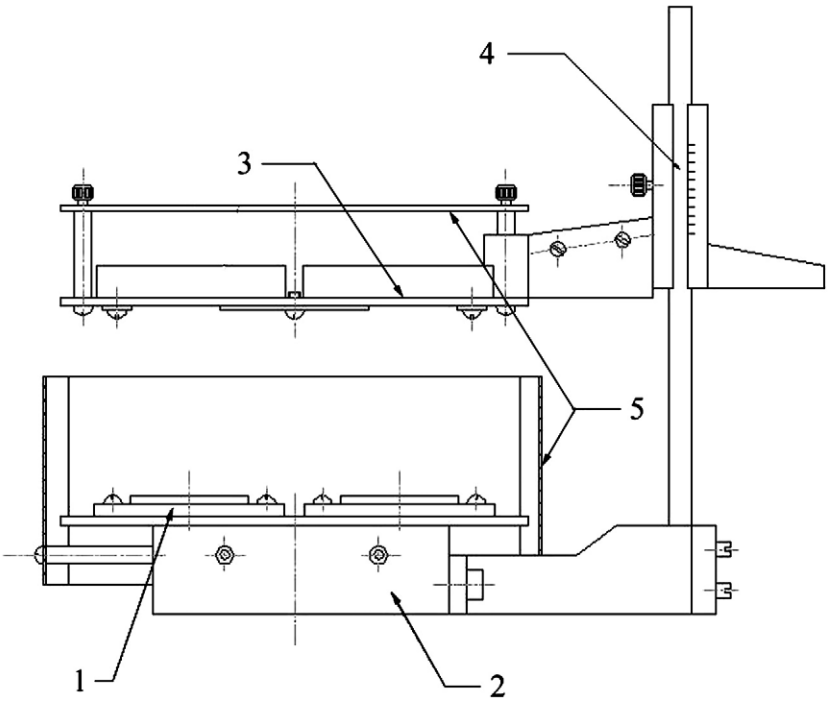

Fig. 1. Sketch map of the structure of the B-field exposure system. 1: array of the permanent magnets, 2: pedestal, 3: loading platform, 4: vernier scale, 5: magnetic shield.

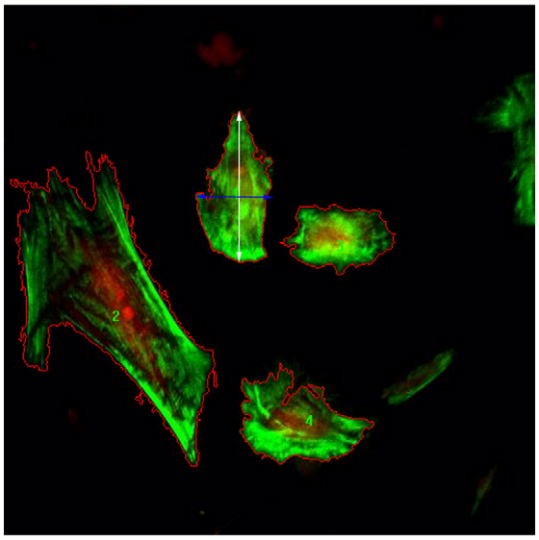

Fig. 2. Image analysis of the LSCM photo of human PDL cells. The area encircled by the red line represents the cross section area of the cell. The white arrowed line and blue line represent the major axis and minor axis of the cell, respectively. (For interpretation of the references to colour in this figure legend, the reader is referred to the web version of this article.)

2.3. Observation of cytoskeleton F-actins and analysis

PDL cells, including the controls, were washed twice with phosphate buffered saline (PBS), fixed with 40g/L paraformaldehyde for 20min, then washed with PBS again. The washed PDL cells were incubated with BODIPY FL phallacidin (1:50, Molecular Probes Inc., Eugene, OR, USA) and BOBO-3 (1:800, Molecular Probes Inc., Eugene, OR, USA) at 37°C for 1h to label F-actin and nucleus, respectively. After washing with PBS, the labeled cells were observed with a laser scanning confocal microscope (LSCM, Model MRC 1024ES, Bio-Rad, UK), using the laser scanning parameters: power 100W, iris 6.2, gain 1139, offset 0. The LSCM photos were analyzed by the LSCM operator with image analysis software (Image-Pro Plus, Version4.5, Media Cybernetics Inc., Silver Spring, MD, USA). For each sample, 4 cells with clear outline in the LSCM photos were selected randomly and automatically image-analyzed, using the built-in software, calculating the cross section area Ac of the cell, cell length (defined along the major axis), the cell width (defined along the minor axis) (Fig. 2).

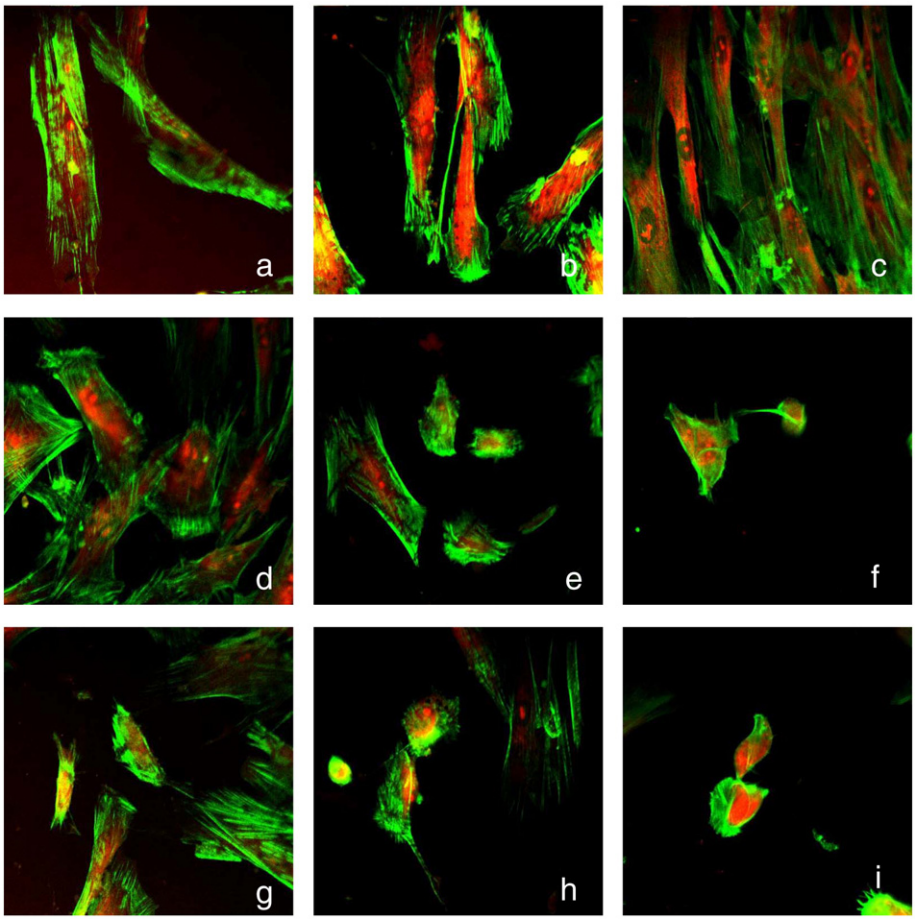

Fig. 3. LSCM photos of the F-actin cytoskeletons of human PDL cells. 600×. a) Control cells 12 h, b) Control cells 36 h, c) Control cells 60 h, d) cells after exposure to $B=10$ mT for 12 h, e): after exposure to $B=10$ mT for 36 h, f) after exposure to 10 mT for 60 h, g) $B=120$ mT for 12 h, h) $B=120$ mT for 36 h, i) $B=10$ mT for 60 h. The cytoskeleton F-actins of PDL cells are represented in green fluorescence and the nuclei in red fluorescence, respectively. (For interpretation of the references to colour in this figure legend, the reader is referred to the web version of this article.)

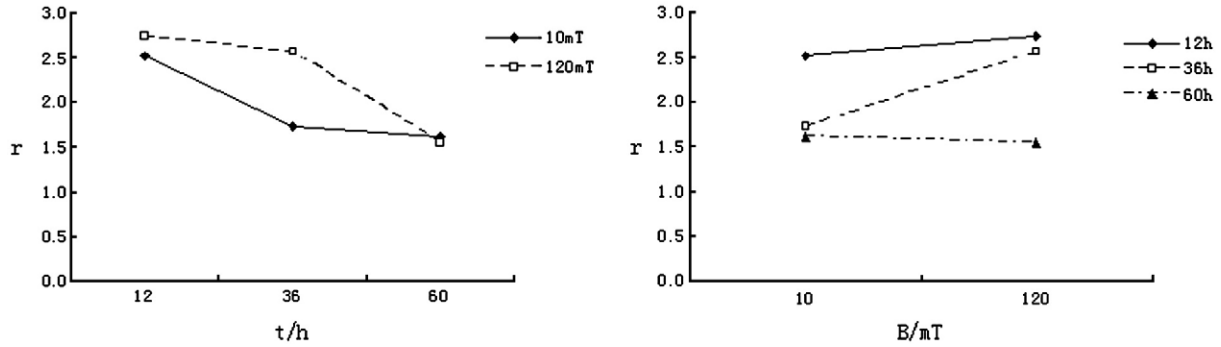

Fig. 4. The length–width ratio r given as a function of exposure time t/h at the given B-field strength and as a function of the B-field, B/mT, at the given exposure time.

The green fluorescence density $f = (F / Fo) / Ac$ in terms of the ratio r of the length L and the width W according to:

$$r = L/W \tag{1}$$

was used in the quantification of the B-field effect on cotoskeleton F-actins. The content of labeled F-actins was quantified by the area integrated optical density, defined as:

$$IOD = fAc(F/Fo)/Ac \tag{2}$$

where F is the fluorescence emission intensity scaled in terms of the apparatus settings relative to the reference Fo. Similar to the Lambert–Beer law of the light attenuation, the fluorescence F is proportional to the concentration of labeled F-actins for not too large absorption of the emitted fluorescence light.

2.4. Statistical analysis

The statistical significance of differences was tested by one-way analysis of variance (ANOVA) followed by the Least-significant difference (LSD) test. Statistical significance was established at the $P < 0.05$ level.

3. Results and discussion

It is recalled that the cytoskeleton elements of eukaryotic cells include microfilaments, microtubules and intermediate filaments, among which the microfilaments predominantly maintain the normal shape of the cell. Actin is the basic component of microfilaments. There are two types of actins: F-actins in filamentous form and G-actins in the free form, in normal cells they are in reactive dynamic balance [28].

For optical monitoring, we labeled the cytoskeleton F-actins of human PDL cells, using the fluorescent dye BODIPY FL phallacidin, which is specifically bound to F-actins. The image analysis software (Image-Pro Plus, Version4.5, Media Cybernetics Inc., Silver Spring, MD, USA) automatically calculates and scales the length–width ratio r, according to Eq. (1) and quantifies the fluorescent F-actins according to Eq. (2). The LSCM photos are shown in Fig. 3.

The cytoskeleton F-actins of control cells were of clearly visible filamentous configuration and were arranged parallel to the long axes of cells (Fig. 3a, b and c). After exposure to B = 10mT for 12h, size and shape of the cells were apparently not changed as compared to those of the control cells. Also, at this condition of low B-field and short exposure time, the cytoskeleton F-actins remained clearly visible and orderly arranged (Fig. 3d). However, at B = 10mT SMF for 36h and 60h, respectively, PDL cells did shrink and the cytoskeleton F-actins became shorter and disordered compared to the controls (Fig. 3e and f). The exposure to B = 10mT and the long exposure time of 60h caused the cells to shrink to an oval shape and the filament configuration of the F-actins can hardly be optically discerned (Fig. 3f).

After exposure to 120mT, cell shrinkage, i.e., shortening and disordering of the structure of the cytoskeleton F-actins is even

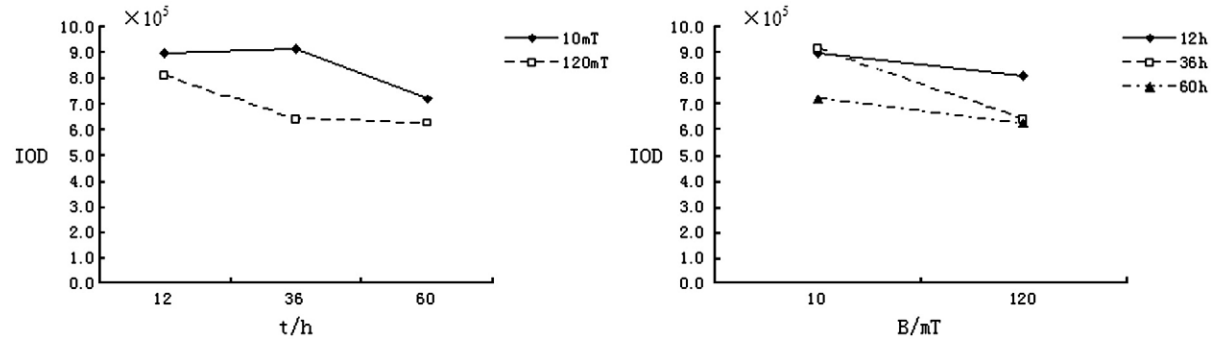

Fig. 5. The IOD given as a function of exposure time t/h at the given B-field strength and as a function of the B-field, B/mT, at the given exposure time.

Table 1
Area Ac of cell cross section (mean±standard deviation, unit: pixel)

Exposure time (h)	Control group	10 mT group	120 mT group	*P*-value
12	23052±10938	19304±5455	12615±8269	0.266
36	18397±5851	11239±9070	7523±3767	0.113
60	19316±2977	6941±3607[a]	5673±2048[a]	0.000
P-value	0.652	0.064	0.222	

[a] $P<0.05$, vs control group.

more evident (Fig. 3g, h, and i). Under the extreme condition of 120mT for 60h, the configuration of the F-actins within the shrunken cells was not discernable anymore (Fig. 3i).

These observations suggest that the targets of the *B*-field forces are the cytoskeleton F-actins. The *B*-field induced structural changes of the filaments obviously precede the changes of the overall cell shape.

The length–width ratio r and IOD given as a function of exposure time *t* / *h* at the given *B*-field strength, and, too, as a function of the *B*-field, *B*/mT, at the given exposure time, are shown in Figs 4 and 5 respectively.

For both the *B* = 10mT and *B* = 120mT exposure cells, the length–width ratio *r* decreased with the exposure time *t*/*h* increased (Fig. 4), consistent with the concept that amplification and accumulation effects are the basis of the effects of EMFs [31]. The IOD did not change much with the exposure time *t*/*h* and *B*-field *B*/mT increased (Fig. 5).

Statistical analysis of the image data revealed differences in the cross section area Ac, concomitant with changes in the r values and the IOD values, indicative for changes in the content of the F-actins (Tables 1–3).

Overall, the optical results suggest that the cell shape changes before the cross section is reduced by shrinkage due to contraction of the cytoskeleton microfilaments. The IOD values of F-actins as a function of the *B*-field intensity and exposure time are consistent with the concept that it is primarily the contraction of the F-actin filaments, and not the disassembly of the F-actins, that are causative for the observed geometrical changes.

It is reported that in another "in vitro" system with the human malignant melanoma cells, the exposure to very large *B*-fields in the range $0.5 \le B/T \le 4.7$ decreases the ability of cells to remain adherent to the surface of culture dish. It was suggested that the reduction in adherence is caused by a field-induced structural change in the integrin molecules located on the cell surfaces. This structure is presumed to subsequently affect the transmembrane signal transduction, finally leading to a decrease in the cellular adhesive ability [32]. Here, the shrinkage of the treated cells to oval forms indicate, too, a reduction in the adhering ability of cells.

Table 2
Length/width ratio, *r*, of the PDL cells (mean±standard deviation)

Exposure time (h)	Control group	10 mT group	120 mT group	*P*-value
12	4.5369±0.7023	2.5030±0.5409[a]	2.7248±0.4102[a]	0.001
36	4.9919±1.6752	1.7235±0.3725[a, b]	2.5510±1.6179[a]	0.020
60	6.1003±0.9345	1.6039±0.1294[a, b]	1.5430±0.4008[a]	0.000
P- value	0.211	0.019	0.244	

[a] $P<0.05$, vs control group; [b] $P<0.05$, vs 12 h group.

Table 3
Integrated optical density (IOD, mean±standard deviation) of cytoskeleton F-actins

Exposure time (h)	Control group	10 mT group	120 mT group	*P*-value
12	1880055±741192	895295±561062[a]	804371±178605[a]	0.039
36	1300155±224983	911181±386399	635167±351148	0.053
60	1159661±367843	716858±373194	621039±306870	0.122
P-value	0.148	0.798	0.622	

[a] $P<0.05$, vs control group.

In further conclusion, if our "in vitro" cell data can be projected on to the *B*-field treatments of humans, there is a potential health risk for high *B*-fields and very long exposure time for patients exposed to open-field dental magnetic attachments. On the same line, also closed-field magnetic attachments should be carefully designed and manufactured to reduce the stray fields (flux leakage) to minimize adverse effects.

Acknowledgements

We gratefully acknowledge editorial advice and financial support by grants for applied and fundamental scientific research from Sichuan Province, China (no. 02sy029.138) and by Shanghai Leading Academic Discipline Project (project number: T0202).

References

[1] J. Wiskirchen, E.F. Gronewaller, F. Heinzelmann, R. Kehlbach, E. Rodegerdts, M. Wittau, H.P. Rodemann, C.D. Claussen, S.H. Duda, Human fetal lung fibroblasts: in vitro study of repetitive magnetic field exposure at 0.2, 1.0, and 1.5 T, Radiology 215 (2000) 858–862.
[2] A.A. Pilla, Low-intensity electromagnetic and mechanical modulation of bone growth and repair: are they equivalent? J. Orthop. Sci. 7 (2002) 420–428.
[3] P.J. Sandler, S. Meghji, A.M. Murray, S.D. Springate, J.R. Sandy, V. Crow, R.T. Reed, Magnets and orthodontics, Br. J. Orthod. 16 (1989) 243–249.
[4] J.H. Noar, R.D. Evans, Rare earth magnets in orthodontics: an overview, Br. J. Orthod. 26 (1999) 29–37.
[5] M.A. Riley, A.D. Walmsley, I.R. Harris, Magnets in prosthetic dentistry, J. Prosthet. Dent. 86 (2001) 137–142.
[6] N. Wertheimer, E. Leeper, Adult cancer related to electrical wires near the home, Int. J. Epidemiol. 11 (1982) 345–355.
[7] D.A. Savitz, E.E. Calle, Leukemia and occupational exposure to electromagnetic fields: review of epidemiologic surveys, J. Occup. Med. 29 (1987) 47–51.
[8] M. Feychting, A. Ahlbom, Magnetic fields, leukemia, and central nervous system tumors in Swedish adults residing near high-voltage power lines, Epidemiology 5 (1994) 501–509.

[9] M. Feychting, F. Jonsson, N.L. Pedersen, A. Ahlbom, Occupational magnetic field exposure and neurodegenerative disease, Epidemiology 14 (2003) 413–419.
[10] J.A. Evans, D.A. Savitz, E. Kanal, J. Gillen, Infertility and pregnancy outcome among magnetic resonance imaging workers, J. Occup. Med. 35 (1993) 1191–1195.
[11] N.C. Blumenthal, J. Ricci, L. Breger, A. Zychlinsky, H. Solomon, G.G. Chen, D. Kuznetsov, R. Dorfman, Effects of low-intensity AC and/or DC electromagnetic fields on cell attachment and induction of apoptosis, Bioelectromagnetics 18 (1997) 264–272.
[12] A. Linder-Aronson, S. Lindskog, Effects of static magnetic fields on human periodontal fibroblasts in vitro, Swed. Dent. J. 19 (1995) 131–137.
[13] J. Sabo, L. Mirossay, L. Horovcak, M. Sarissky, A. Mirossay, J. Mojzis, Effects of static magnetic field on human leukemic cell line HL-60, Bioelectrochemistry 56 (2002) 227–231.
[14] D. Flipo, M. Fournier, C. Benquet, P. Roux, C. Le Boulaire, C. Pinsky, F.S. LaBella, K. Krzystyniak, Increased apoptosis, changes in intracellular Ca^{2+}, and functional alterations in lymphocytes and macrophages after in vitro exposure to static magnetic field, J. Toxicol. Environ. Health A 54 (1998) 63–76.
[15] M.J. Azanza, A. del Moral, Isolated neuron amplitude spike decrease under static magnetic fields, J. Magn. Magn. Mater. 157/158 (1996) 593–594.
[16] M. Hiraoka, J. Miyakoshi, YP. Li, B. Shung, H. Takebe, M. Abe, Induction of *c-fos* gene expression by exposure to a static magnetic field in HeLaS3 cells, Cancer Res. 52 (1992) 6522–6524.
[17] V.R. Narra, R.W. Howell, S.M. Goddu, D.V. Rao, Effects of a 1.5-Tesla static magnetic field on spermatogenesis and embryogenesis in mice, Invest. Radiol. 31 (1996) 586–590.
[18] M.M. Atef, M.S. Abd el-Baset, A. el-Kareem, S. Aida, M.A. Fadel, Effects of a static magnetic field on haemoglobin structure and function, Int. J. Biol. Macromol. 17 (1995) 105–111.
[19] Y. Watanabe, M. Nakagawa, Y. Miyakoshi, Enhancement of lipid peroxidation in the liver of mice exposed to magnetic fields, Ind. Health 35 (1997) 285–290.
[20] A. Linder-Aronson, S. Lindskog, P. Rygh, Orthodontic magnets: effects on gingival epithelium and alveolar bone in monkeys, Eur. J. Orthod. 14 (1992) 255–263.
[21] L. Bondemark, J. Kurol, A. Wennberg, Orthodontic rare earth magnets–in vitro assessment of cytotoxicity, Br. J. Orthod. 21 (1994) 335–341.
[22] N. Prasad, E. Lotzova, J.I. Thornby, K.H. Taber, The effects of 2.35-T MR imaging on natural killer cell cytotoxicity with and without interleukin-2, Radiology 175 (1990) 261–263.
[23] A. Mahdi, P.A. Gowland, P. Mansfield, R.E. Coupland, R.G. Lloyd, The effects of static 3.0 T and 0.5 T magnetic fields and the echo-planar imaging experiment at 0.5 T on *E. coli*, Br. J. Radiol. 67 (1994) 983–987.
[24] S. Camilleri, F. McDonald, Static magnetic field effects on the sagittal suture in *Rattus norvegicus*, Am. J. Orthod. Dentofac. Orthop. 103 (1993) 240–246.
[25] L. Bondemark, J. Kurol, A. Larsson, Human dental pulp and gingival tissue after static magnetic field exposure, Eur. J. Orthod. 17 (1995) 85–91.
[26] C. Xu, Y.L. Chao, L. Du, L. Yang, Measurements of the flux densities of static magnetic fields generated by two types of dental magnetic attachments and their retentive forces, J. Sichuan Univ. (Med. Sci. Edi.) 35 (2004) 412–415.
[27] C. Xu, Y.L. Chao, W.C. Liu, Z. Fan, F.Q. Zhang, Biological effects of static magnetic field of dental magnetic attachments, J. Dent. Res. 84 (Spec Iss A) (2005) 1601.
[28] T. Akisaka, H. Yoshida, S. Inoue, K. Shimizu, Organization of cytoskeletal F-actin, G-actin, and gelsolin in the adhesion structures in cultured osteoclast, J. Bone Miner. Res. 16 (2001) 1248–1255.
[29] L. Zhang, L. Zhou, A. Vega-Gonzalez, D. Mendoza, R Drucker-Colin, Extremely low frequency magnetic fields promote neurite varicosity formation and cell excitability in cultured rat chromaffin cells, Comp. Biochem. Physiol. C Pharmacol. Toxicol. Endocrinol. 118 (1997) 295–299.
[30] L. Bondemark, J. Kurol, A. Wisten, Extent and flux density of static magnetic fields generated by orthodontic samarium-cobalt magnets, Am. J. Orthod. Dentofac. Orthop. 107 (1995) 488–496.
[31] E. Neumann, Digression on chemical electromagnetic field effects in membrane signal transduction-cooperativity paradigm of the acetylcholine receptor, Bioelectrochemistry. 52 (2000) 43–49.
[32] W.O. Short, L. Goodwill, C.W. Taylor, C. Job, M.E. Arthur, A.E. Cress, Alteration of human tumor cell adhesion by high-strength static magnetic fields, Invest. Radiol. 27 (1992) 836–840.